OXFORD

SOT | Society of Toxicology
academic.oup.com/toxsci

TOXICOLOGICAL SCIENCES, 173(1), 2020, 156–170

doi: 10.1093/toxsci/kfz213
Advance Access Publication Date: October 25, 2019
Research Article

Early Effects of Cyclophosphamide, Methotrexate, and 5-Fluorouracil on Neuronal Morphology and Hippocampal-Dependent Behavior in a Murine Model

Julie E. Anderson,*,† Madison Trujillo,*,†,§ Taylor McElroy,*,† Thomas Groves,*,†,‡ Tyler Alexander,*,† Frederico Kiffer,*,† and Antiño R. Allen*,†,‡,1

*Division of Radiation Health; †Department of Pharmaceutical Sciences; and ‡Neurobiology & Developmental Sciences, University of Arkansas for Medical Sciences, Little Rock, Arkansas 72205

[1]To whom correspondence should be addressed at University of Arkansas for Medical Sciences, 4301 West Markham, Suite 441B-2, Little Rock, AR 72205. Fax: (501) 526-6599. E-mail: AAllen@uams.edu.

ABSTRACT

Breast cancer (BC) is the most common cancer among women. Fortunately, BC survival rates have increased because the implementation of adjuvant chemotherapy leading to a growing population of survivors. However, chemotherapy-induced cognitive impairments (CICIs) affect up to 75% of BC survivors and may be driven by inflammation and oxidative stress. Chemotherapy-induced cognitive impairments can persist 20 years and hinder survivors' quality of life. To identify early effects of CMF administration in mice, we chose to evaluate adult female mice at 2-week postchemotherapy. Mice received weekly IP administration of CMF (or saline) for 4 weeks, completed behavioral testing, and were sacrificed 2 weeks following their final CMF injection. Behavioral results indicated long-term memory (LTM) impairments postchemotherapy, but did not reveal short-term memory deficits. Dendritic morphology and spine data found increases in overall spine density within CA1 basal and CA3 basal dendrites, but no changes in DG, CA1 apical, or CA3 apical dendrites. Further analysis revealed decreases in arborization across the hippocampus (DG, CA1 apical and basal, CA3 apical and basal). These physiological changes within the hippocampus correlate with our behavioral data indicating LTM impairments following CMF administration in female mice 2-week postchemotherapy. Hippocampal cytokine analysis identified decreases in IL-1α, IL-1β, IL-3, IL-10, and TNF-α levels.

Key words: cyclophosphamide; methotrexate; 5-fluorouracil; hippocampus; cognition.

In 2013, there was an estimated 14 million cancer survivors with nearly one-fourth representing breast cancer (BC) survivors, and it is estimated there will be 70 million cancer survivors worldwide by 2020 (Ganz and Goodwin, 2015; Weiss, 2008). Breast cancer survival rates have been on the rise because the implementation of adjuvant chemotherapy and death rates have dropped 34% since 1990 (DeSantis et al., 2014; Ganz and Goodwin, 2015). As the survivor population increases, there is a greater urgency to further evaluate the long-term effects of chemotherapy and its impact on patients' quality of life. Chemotherapy-induced cognitive impairments (CICIs), colloquially known as "chemobrain," can be a major impediment that survivors face postchemotherapy. Chemotherapy-induced cognitive impairments can be transient or long-term cognitive deficits in learning, memory, attention, processing speed, and executive function following various chemotherapy regimens(Dietrich et al., 2015; Jean-Pierre et al., 2014).

Recent data from our laboratory have demonstrated that administration of cyclophosphamide (CYP) in adult female mice results in learning and memory impairments 7-week postchemotherapy. Mice exhibited impaired long-term memory (LTM) as assessed by the novel object recognition behavioral task, a task reliant on hippocampal functioning. Mice also exhibited dysregulation of hippocampal synaptic plasticity, which is essential for learning and memory. Our laboratory has also identified elevated cytokine levels and compromised dendritic

architecture following 5-fluorouracil (5-FU) administration in aged male mice (Groves et al., 2017). Although the investigation of individual chemotherapeutic agents offers valuable insight, chemotherapy agents are more commonly administered as combination therapy, including doxorubicin and cyclophosphamide (AC); cyclophosphamide, doxorubicin, and 5-fluorouracil (CAF); cyclophosphamide, epirubicin, and 5-fluorouracil (CEF); and cyclophosphamide, methotrexate, and 5-fluorouracil (CMF) (Carlson et al., 2009).

CMF combination chemotherapy was commonly used to treat BC and is thought to be especially damaging to the central nervous system (CNS) in view of the ability of methotrexate (MTX) and 5-FU to cross the blood-brain barrier (BBB) (Dukic et al., 2000; Sakane et al., 1999). In fact, a large clinical study identified impairments in memory, information-processing speed, and psychomotor speed persisting in BC survivors 20-year post-CMF chemotherapy (Koppelmans et al., 2012). *In vivo* rodent studies of CMF-induced cognitive impairments are extremely limited (Briones and Woods, 2011, 2014). In rats, CMF-induced spatial learning and LTM impairment in water maze testing accompanied by decreased cellular proliferation within the hippocampus 3-week postchemotherapy (Briones and Woods, 2011). In a follow-up study, CMF-treated mice demonstrated persistent neuroinflammation up to 4-week postchemotherapy (Briones and Woods, 2014) which can be associated with a loss in cognitive function (Plesnila, 2016; Ramlackhansingh et al., 2011).

Cyclophosphamide, a nonphase specific cytotoxic agent, is commonly used as an anticancer drug. It is composed of a nitrogen mustard group (bis-chloroethylamine) attached to an oxazaphosphorine ring (Arnold et al., 1958). During World War II, mustard gases were observed to reduce peripheral blood lymphocytes, thus leading to the discovery of the cytotoxic properties of nitrogen mustard derivatives (Christakis, 2011; Goodman et al., 1946). Norbert Brock first synthesized CYP in 1958 (de Jonge et al., 2005; Madondo et al., 2016), and in 1959, it was the eighth cytotoxic anticancer agent approved by the FDA (Emadi et al., 2009). Due to its cytotoxic and immunomodulatory properties, CYP has numerous uses including treatment of lymphoma, leukemia, retinoblastoma, neuroblastoma, and carcinomas of the breast, ovary, endometrium, and lung (Awad and Stuve, 2009; de Jonge et al., 2005). Cyclophosphamide can also be used to treat rheumatoid arthritis, multiple sclerosis, and in preparation for and following transplantations to prevent graft rejection and graft versus host disease (Dollery, 1999; Luznik et al., 2010). In general, CYP can be administered intravenously or orally and has good peripheral bioavailability (de Jonge et al., 2005). Cyclophosphamide can partially penetrate the CNS parenchyma and BBB (Awad and Stuve, 2009; Genka et al., 1990). Conventional chronic and single high-dose administration of CYP has been found to reduce proliferation in the hippocampus (Janelsins et al., 2010), but several studies have failed to find excessive CYP or metabolite presence in the CNS (Genka et al., 1990; Yule et al., 1997).

Methotrexate, another commonly used chemotherapeutic agent, is an antimetabolite. Antimetabolites are classified as agents which inhibit the function of a metabolite, often by having a similar structure to naturally occurring biochemicals. The door to chemotherapeutic research opened following the successful treatment of non-Hodgkin's lymphoma with nitrogen mustard derivative, mustine. Upon observation that folic acid stimulated acute lymphoblastic leukemia cells, Dr Sidney Farber synthesized a folate analog named amethopterin, known today as MTX. Methotrexate, an antifolate, functions through disruption of the metabolic pathway of folic acid (Hess and Khasawneh, 2015; Treatment of Solid Tumor Cancers with the Chemotherapy Drug Methotrexate, 2014). Folic acid, or vitamin B9, is a critical B vitamin that enables cellular replication and proper brain functioning. Folic acid deficiency is associated with high blood levels of homocysteine which is linked to increased risk of arterial disease, dementia, and Alzheimer's disease (Malouf et al., 2003).

Another commonly used chemotherapeutic drug is 5-FU. 5-fluorouracil is also an antimetabolite, like MTX, that interrupts nucleic acid synthesis. In 1954, pyrimidine uracil usage was found to be elevated within rat tumors (Diasio and Harris, 1989; Rutman et al., 1954). As uracil is essential for nucleic acid synthesis, interruption of uracil function was proposed to halt tumor growth. In 1957, uracil analog 5-FU was synthesized. 5-fluorouracil is identical in structure to uracil except for a substitution of the hydrogen on the 5′ carbon of uracil for fluorine (Diasio and Harris, 1989; Duschinsky et al., 1957). 5-fluorouracil works dually by inhibiting thymidylate synthase (TS) and incorporating into RNA and DNA. 5-fluorouracil enters the cell through facilitated transport, like uracil, where it is converted to three primary active metabolites: fluorodeoxyuridine monophosphate, fluorodeoxyuridine triphosphate, and fluorouridine triphosphate (Longley et al., 2003). Though it was introduced nearly half a century ago, 5-FU remains in use today both alone and in combination. It is used notably for solid tumors including breast, gastrointestinal, ovarian, head, neck and noninvasive basal cell carcinomas (Carrillo et al., 2015; Diasio and Harris, 1989). 5-fluorouracil is known to cross the BBB through passive diffusion and induce inflammation in peripheral tissue, the CNS is left vulnerable to neurotoxicity following exposure (Logan et al., 2008; Lyons et al., 2011; Mustafa et al., 2012; Wigmore et al., 2010). In particular, 5-FU accumulation was high in cerebellum leading to cerebellar deficits, such as ataxia, dysarthria, dysmetria, extraocular muscle abnormalities, optic nerve neuropathy and extrapyramidal damage (Peddi et al., 2014; Riehl and Brown, 1964). The aim of this study is to determine the extent to which combined cyclophosphamide, MTX, and 5-FU affect hippocampal-dependent behavior and neuronal morphology.

MATERIALS AND METHODS

Animals

Six month-old female C57Bl6/J mice ($N = 30$) were purchased (Jackson Laboratory). The mice were group housed ($n = 5$/cage) under a constant 12-h light:12-h dark cycle in a climate-controlled environment. Food and water were provided *ad libitum*. Body weights and food intake were measured weekly. Mice housed together were the same treatment group and allowed one week of acclimation prior to injections. All procedures were approved by the Institutional Animal Care and Use Committee at the University of Arkansas for Medical Sciences (Little Rock, Arkansas).

Chemotherapeutic Paradigm

Mice received intraperitoneal (IP) injections weekly for 4 weeks of either saline (0.9% sodium chloride) or CMF (60, 4 , and 60 mg/kg, respectively). All mice received a total of four administrations (Days 1, 8, 15, and 22). Cyclophosphamide, MTX, and 5-Fu were all purchased from UAMS Inpatient Pharmacy. Drugs were diluted with sterile saline and stored per the manufacturer's instructions. Drugs were mixed immediately prior to injections.

Behavioral Scheme

Y-maze. Mice were handled 5 days prior to the onset of behavioral testing. Prior to each day of testing, mice were acclimated to the testing room in their home cage for 1 h. Mice first completed a Y-maze task to assess short-term spatial memory and exploratory activity. They were exposed in two trials to an apparatus composed of three arms: start, familiar, and novel (Gottlieb et al., 2006). Each clear, acrylic arm (45 ×15 × 30 cm) of the Y-maze contains a unique visual cue affixed at the end of the arm. The Y-maze is based on the instinctive curiosity of rodents to explore novel stimuli without positive or negative reinforcement (Dellu et al., 1992). In the first trial (ie, training trial), mice were introduced in the start arm (facing the end of the arm) and allowed to explore the start and familiar arms for 5 min; the novel arm was blocked during the initial training trial. After a 4-h intertrial interval, the mice were reintroduced to the Y-maze for the second trial (ie, testing trial) and allowed to explore all three arms for 5 min. As rodents naturally orient their head toward novel stimuli, this orienting response should habituate following subsequent exposure given intact learning and memory domains (Honey et al., 1998). Thus, cognitively intact mice should preferentially explore the novel arm. Allocation of arms was counterbalanced across trials. A CCD video camera was located above the maze for automatic behavioral analysis using EthoVision XT video tracking system (Noldus Information Technology, Leesburg, Virginia). The arena was cleaned with 20% ethanol between every trial.

Morris water maze. Hippocampal-dependent spatial learning and memory were assessed via the Morris water maze (MWM). A circular pool (diameter, 140 cm) was filled with temperature-controlled (24°C) opaque water, and the mice were trained to locate a platform. Morris water maze is a 5-day task during which the mice are required to find either a visible (days 1–2) or hidden platform (days 3–5) on the basis of extra-maze cues (Benice et al., 2006). For visible-platform days, the platform was moved to a different quadrant of the pool for each session. For hidden-platform days, the platform did not change quadrants.

Each day, there were two sessions with a 2-h intertrial interval, and each session consisted of three trials with a 10-min intertrial interval. Mice were placed into the water, facing the edge of the pool in one of nine randomized start locations, which was changed for each trial. Trials ended when a mouse located the platform or after 60 s. If a mouse failed to locate the platform, it was led to the platform by the experimenter and allowed to sit on platform for 10 s. A CCD video camera was located above the maze for recording and automatic tracking using the EthoVision XT video tracking system, which was set at 6 samples per second.

To measure spatial memory retention, probe trials were conducted following the third session on days 3–5. For the probe trial, the hidden platform was removed from the pool. Mice were placed in the quadrant opposite the target quadrant (previous location of the hidden platform) and allowed to swim for 60 s. The time spent in the target quadrant was compared with that spent in the three nontarget quadrants. Average velocity and distance to platform are also used as measures of performance (Allen et al., 2014). After the final probe trial on day 5, mice were immediately sacrificed.

Tissue Preparation

Mice were sacrificed 2 weeks following their final CMF administration which correlated with their final day of MWM. Mice were sacrificed 30 min following the probe trial on the final day of MWM. All mice were cervically dislocated and brains were divided longitudinally by hemisphere flash-frozen on liquid nitrogen, and stored at −80°C. Right hemispheres were immediately submerged into potassium dichromate and mercuric chloride (Solution A) from the superGolgi kit (Bioenno Tech, Santa Ana, California) for Golgi-Cox staining.

Molecular Assays

Golgi-Cox staining. For Golgi-Cox staining, all steps were carried out in a light-protected container. Whole brains were immediately subjected to potassium dichromate and mercuric chloride (Solution A) from the superGolgi kit (Bioenno Tech, Santa Ana, California). Solution A impregnated the brains for 11 days at room temperature. After impregnation, brains were incubated in postimpregnation buffer (Solution B) for 2 days at room temperature. Brains were sectioned into 200-μm sections in cold PBS with a vibrating microtome and placed into 24-well plates. Sections are rinsed with PBS–Triton X-100 (PBS-T) for 30 min at room temperature and then stained with ammonium hydroxide (Solution C) for 19 min at room temperature. Then sections were incubated with poststaining buffer (Solution D) for 19 min at room temperature followed by PBS–T washes (3× for 10 min). Sections were mounted onto 1% gelatin-coated slides and allowed to dry overnight. Slides were dehydrated with 100% ethanol (3× for 5 min) followed by clearing in xylene (3× for 5 min). Last, slides were cover-slipped with Permount mounting medium (Fisher Scientific, SP15).

Dendritic spine density and morphology. We analyzed dendritic spines in coded Golgi-impregnated brain sections from the dorsal and ventral hippocampus. Spines were examined on dendrites of dorsal dentate gyrus (DG) granule neurons and on apical (stratum radiatum) and basal (stratum oriens) dendrites of the dorsal CA1and CA3 pyramidal neurons. The neurons that satisfied the following criteria were chosen for analysis in each of the experimental groups: (1) presence of nontruncated dendrites; (2) consistent and dark Golgi-staining along the extent of the dendrites; and (3) relative isolation from neighboring neurons to avoid interference with analysis (Titus et al., 2007). Five dendritic segments per neuron were analyzed (each at least 20 nm long), and 6–7 neurons were analyzed per brain (Magariños et al., 2011). Neurons that met staining criteria were traced using a 100× oil objective, a computerized stage, and Neurolucida software (Ver. 11, Microbrightfield, Inc.).

Spine analyses were based on the method of Margarinos et al. (2011), Tada et al. (2000), Magariños et al. (2011) which focuses on spines that are parallel to the plane of section. Although the method may underestimate the total number of spines, it facilitates a direct comparison of treatment groups when they are analyzed in an identical manner (Tada et al., 2000). ImageJ software was used to calculate linear spine density (Spires-Jones et al., 2011). Three morphological classes of dendritic spines were classified, with the name of each class based on their size and shape: (1) mushroom spines, which have complex postsynaptic densities with more glutamate receptors than other spines (Bourne and Harris, 2008); (2) stubby spines, which lack a stem; and (3) thin spines, which consist of a protracted, narrow stem and a globular head (Lai and Ip, 2013). The dendritic spine volume is used in part to define them, with thin spines generally smaller (0.01 μm^3) compared with mushroom spines (0.8 μm) (Harris, 1999; Harris and Kater, 1994).

Dendritic morphology quantification. Dendritic morphological characteristics included Sholl analysis, total dendritic length,

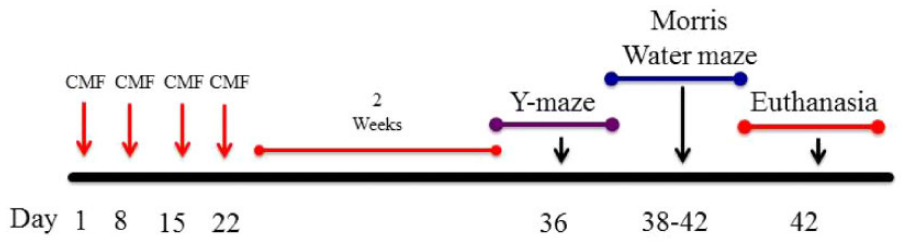

Figure 1. Schematic diagram showing experimental design. Four-month-old C57BL/6J Female mice received intraperitoneal injections weekly for 4 weeks of either saline (0.9% sodium chloride) or CMF. Two weeks after last injections, behavioral testing was initiated.

number of branch points, ends, and dendritic complexity which were performed using the Neuroexplorer component of the Neurolucida program (Microbrightfield, Inc., Version 11; Williston, Vermont). Sholl analysis represents the amount and distribution of the dendritic arbor, assessing increasing distances (20 μm) from the soma of the neuron (Sholl, 1953). The length of the dendritic branch within each progressively larger circle is counted extending outward from the soma (Vollala et al., 2011). Branch points, the bifurcations within the dendrites, was also analyzed as a measure of dendritic arborization. Dendritic complexity was determined by the following equation, Complexity = Σ (branch tip orders + No. branch tips) × (total dendritic length/total number of primary dendrites). In the CA1 and CA3, we analyzed apical and basal dendrites separately.

Cytokine and chemokine analysis. Hippocampi were homogenized individually in 200 μl PBS (Roche, Switzerland) containing Complete Protease Inhibitor (Roche) using a Kontes cordless pestle at 4°C. Homogenized samples were centrifuged at 500 × g at 4°C for 10 min. Supernatants were transferred to new Eppendorf tubes on ice and centrifuged at 15,000 × g at 4°C for 5 min. Supernatants were collected and shipped to Quansys Biosciences (Logan, Utah) for analysis with Q-Plex Array kits for mouse cytokines: IL-1α, IL-1β, IL-2, IL-3, IL-4, IL-5, IL-10, IL-12p70, MCP-1, TNF-α; GMCSF; and RANTES (Figures 1 and 2). All cytokine data are expressed as pg/mL protein.

Statistical Analysis

Two-way ANOVAs with Holm-Sidak's multiple comparison tests were used to analyze body weights and food consumption at each week. Unpaired two-tailed *t*-tests with Welch's correction were used to evaluate statistical differences between control and CMF-treated mice. One-way or two-way analysis of variance (ANOVA) followed by Bonferroni's post-hoc was used when appropriate in behavioral assays. All outliers were excluded by the ROUT method (Motulsky and Brown, 2006). Data are expressed as mean ± SEM, and $p < .05$ was considered significant. All statistical analyses were conducted using GraphPad Prism 6.0 software (La Jolla, California).

RESULTS

CMF: 2-Week Postchemotherapy

A total of N = 20 mice were assigned to the 2-week postchemotherapy group. Mice received weekly IP injections of saline ($n = 10$) or CMF ($n = 10$) for 4 weeks (days 1, 8, 15, 22). Two weeks after the last CMF injection, mice completed Y-Maze and MWM (Figure 3).

Food Consumption and Body Weight

Food consumption and body weights were tracked during injections and 2 weeks after, no significant changes in food consumption were identified ($F_{(3,\ 6)} = 1.65$, $p = .27$; Figure 4A). For body weight, there were a significant differences between treatment-by-week interaction ($F_{(5,\ 90)} = 10.86$, $p < .0001$; Figure 4B), but there was no significant difference between treatments ($F_{(1,\ 18)} = 0.007$, $p = .93$; Figure 4B). Additionally, post-hoc analysis did not reveal any significant changes in body weights.

Y-Maze

To assess short-term spatial memory and exploratory activity, mice completed Y-maze testing. Rodents will naturally orient towards a novel stimulus, preference for the novel arm represents normal spatial recognition. Both the saline-treated ($F_{(2,\ 26)} = 17.22$, $p < .0001$; Figure 5A) and CMF-treated ($F_{(2,\ 27)} = 16.85$, $p < .0001$; Figure 5B) mice significantly preferred exploration of the novel arm compared with the familiar and start arms.

Morris Water Maze

Following Y-Maze, spatial learning and memory was assessed with 5-day MWM testing. A decrease in path length (ie, distance moved) to the platform represents improvement in spatial learning and memory. Repeated measures ANOVA of distance traveled revealed no significant differences in treatment-by-day interactions ($F_{(4,\ 90)} = 0.11$, $p = .98$). In addition, velocity revealed no significant differences in treatment-by-day interactions ($F_{(4,\ 90)} = 1.48$, $p = .22$), but did reveal a significant treatment effect ($F_{(1,\ 90)} = 7.37$, $p < .01$; Figure 6A). Post-hoc analysis revealed a significant difference on day 5 ($p < .05$; Figure 6A).

For probe trial days, the platform was removed after hidden platform training on days 3-5 to assess spatial memory retention. Intact animals are expected to demonstrate spatial memory retention by spending more time in the target quadrant compared with the other quadrants. In our 2-week postchemotherapy mice, the saline-treated mice statistically spent more time in the target quadrant compared with the right, opposite, and left quadrants on the first probe day (day 3) ($F_{(3,\ 32)} = 7.83$, $p < .001$; Figure 7A). In contrast, CMF-treated mice did not spend more time in the target quadrant compared with other quadrants ($F_{(3,\ 36)} = 2.70$, $p = .06$; Figure 7B).

On day 4, the saline-treated mice statistically spent more time in the target quadrant compared with the right, opposite, and left quadrants ($F_{(3,\ 32)} = 11.22$, $p < .0001$; Figure 7C). In CMF-treated mice there was a statistical difference in the percentage of time spent among the quadrants ($F_{(3,\ 35)} = 3.42$, $p < .05$; Figure 7D); however, post-hoc analysis only revealed a statistical difference in time spent in one quadrant when comparing to

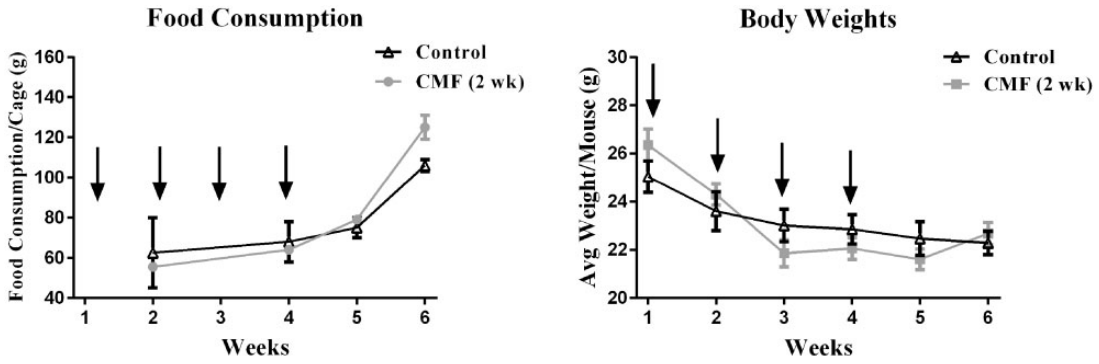

Figure 2. Food Consumption & Body Weight. Black arrows indicate saline or CMF injections. Food consumption is shown as grams (g) of food consumed per cage. (a & b) There were no changes in body weights and food consumption during chemotherapy or 2-week post-injection (N=20). Error bars represent mean ± SEM.

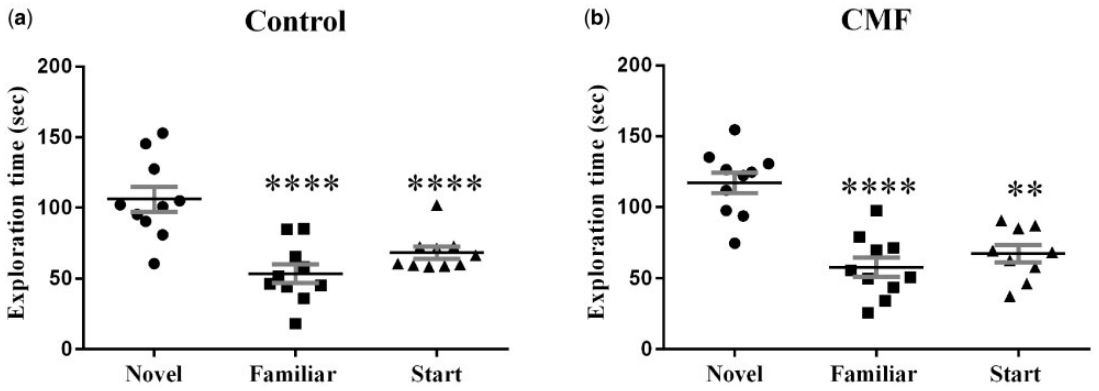

Figure 3. Y-maze. Both control (saline-treated) and CMF-treated groups spent significantly more time exploring the novel arm during the testing phase of the Y-maze, indicating no short-term memory deficits. Error bars are mean ± SEM ($n = 10$); ***P <.001; ****P <.0001.

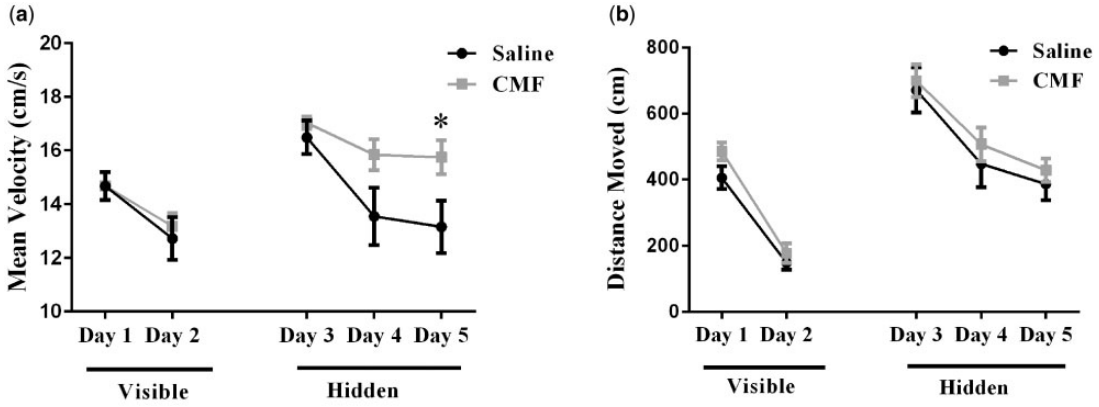

Figure 4. Distance moved to the target platform during visible and hidden training sessions a) Analysis revealed an effect of treatment, in mice that received CMF swam significantly faster day 5 to reach the platform. b) During the visible-platform training (days 1 and 2), all experimental groups swam similar distances to the platform. All groups showed daily improvements in their ability to locate during the hidden-platform training (days 3–5). Mean ± SEM ($n = 10$); *P < 0.05.

the target quadrant ($p < .05$; Figure 7D). CMF-treated mice did not spend more time in the target quadrant compared all other quadrants.

During the final probe trial (day 5), the saline-treated mice statistically spent more time in the target quadrant compared with the right, opposite, and left quadrants ($F_{(3,\ 32)} = 18.33$, $p < .0001$; Figure 7E). Similarly, CMF-treated mice also spent more time in the target quadrant compared with the right, opposite and left quadrants ($F_{(3,\ 36)} = 8.15$, $p < .001$; Figure 7F). With continued training, CMF-treated mice were able to successfully learn the location of the platform by day 5.

Changes in Dendritic Spine Density and Morphology

Dentate gyrus granule neurons. The quantitative analysis showed that overall spine density in the DG after CMF treatment was not significantly changed ($t = 0.47$, $p = .64$; Table 1). Next, we analyzed the density of different types of dendritic spines, finding that the density of thin spines were not significantly modulated ($t = 0.99$, $p = .35$; Table 1). However, in the DG, we observed a significant increase in the number of stubby spines ($t = 2.80$, $p < .05$; Table 1) and a decrease in the number of mushroom spines in CMF-treated animals compared with controls ($t = 4.50$, $p < .01$; Table 1).

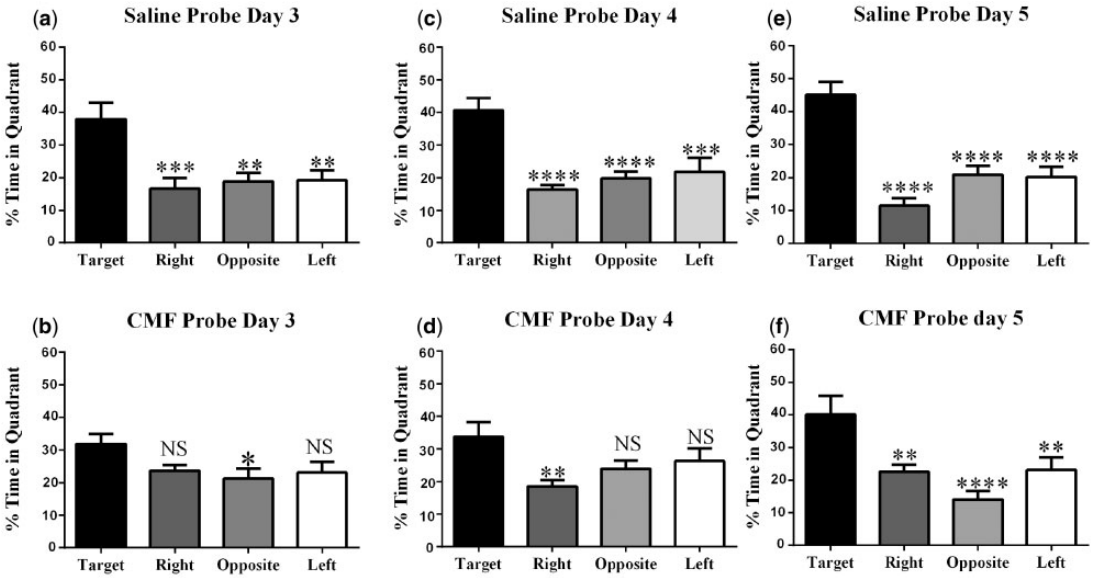

Figure 5. Spatial memory retention during probe trials on days 3–5 of Morris water-maze testing. (a, c, and e) Saline probe trials; saline-treated animals spent significantly more time in the target quadrant than other quadrants. (b) Day 3 CMF-treated mice did not discriminate between the target, right and left quadrant. (d) Day 4 CMF-treated mice were unable to distinguish target, opposition and left quadrant. (f) Day 5 CMF treated animals spent significantly more time in the target quadrant than other quadrants. Each bar represents the mean of 10 mice; error bars are the SEM. *$P < .05$; ***$P < .001$; ****$P < .0001$.

CA1 pyramidal neurons. Similar to what was observed in the DG spine analysis, CMF-treatment did not significantly modulate overall density in the CA1 apical spines (apical: $t = 1.59$, $p = .43$; Table 2). In addition, when we analyzed the density by spine type, we did not find significant changes in thin ($t = 1.49$, $p = .18$; Table 2), stubby ($t = 0.95$, $p = .37$; Table 2) or mushroom ($t = 1.58$, $p = .15$; Table 2) spine types. In CA1 basal, there was a significant increase in spine density when CMF-treated animals were compared with controls ($t = 1.60$, $p < .05$; Table 2). When we analyzed spine type we also found no significant changes in thin ($t = 1.00$, $p = .34$; Table 2), stubby ($t = 0.42$, $p = .68$; Table 2) or mushroom spines ($t = 2.02$, $p = .07$; Table 2).

CA3 pyramidal neurons. In the CA3 apical pyramidal dendrites, there were no significant changes in the overall density of spine (apical: $t = 1.68$, $p = .13$; Table 3). When we analyzed spine type we also found no significant changes in thin ($t = 0.67$, $p = .52$; Table 3), stubby ($t = 0.12$, $p = .91$; Table 3) or mushroom spines ($t = 1.44$, $p = .18$; Table 3). In the CA3 basal, there was an increase in spine density ($t = 2.58$, $p < .05$; Table 3). However similar to the apical spines, there were no significant changes in thin ($t = .60$, $p = .56$; Table 3), stubby ($t = 0.44$, $p = .67$; Table 3) or mushroom spines ($t = 0.26$, $p = .80$; Table 3).

Changes in Dendritic Morphology in Granular Neurons of the Dentate Gyrus

Dentate gyrus granule neurons. To further investigate the effects of CMF-treatment on dendrite morphology we performed a segmental Sholl analysis to examine the changes in dendritic length. In the DG, there was a significant interaction between treatment and segmental dendritic length after CMF-treatment ($F_{(28,\ 116)} = 2.88$ $p < .001$; Figure 8A). The ANOVA also detected a significant main effect of treatment ($F_{(1,\ 116)} = 191.4$; $p < .0001$) and distance ($F_{(28,\ 116)} = 118$; $p < .0001$). Post-hoc analysis (Holm-Sidak) revealed that CMF-treatment decreased dendritic arborization compared with the sham controls. We observed significant decreases in the dendritic length from 100 to 190 μm from the soma (Figure 8A). In addition, we observed significant decreases in the number of branch points ($t = 4.32$, $p < .05$; Table 1), dendritic ends ($t = 4.87$, $p < .01$; Table 1), dendritic length ($t = 10.65$, $p < .001$; Table 1), and dendritic complexity ($t = 3.70$, $p < .05$; Figure 8B) in CMF-treated animals compared with saline-treated. These data indicate that CMF decreased dendritic complexity in the DG region of the hippocampus.

CA1 pyramidal neurons. We performed a similar analysis on the apical and basal region of the CA1 pyramidal neurons. There was a significant interaction between treatment and segmental dendritic length in the CA1 apical area ($F_{(28,\ 116)} = 2.08$: $p < .01$; Figure 9A). A two-way ANOVA also detected a significant main effect of treatment ($F_{(1,\ 116)} = 136.7$: $p < .0001$) and distance ($F_{(28,\ 116)} = 62.86$; $p < .0001$). Post-hoc analysis (Holm-Sidak) revealed that CMF-treatment decreased dendritic arborization compared with the sham controls. We observed significant decreases in dendritic length in the apical region of CA1 70 and 100–190 μm (Figure 9A) away from the soma.

In the basal dendrites of CA1 pyramidal cells, there was a significant interaction between treatment and sham segmental dendritic length ($F_{(28,\ 116)} = 1.84$; $p < .05$; Figure 9C). The ANOVA also detected a main effect of treatment ($F_{(1,\ 116)} = 24.71$; $p < .001$) and distance ($F_{(28,\ 116)} = 246.5$; $p < .0001$). Post-hoc analysis (Holm-Sidak) revealed that CMF decreased dendritic arborization at 70 μm from the soma as well as at 100 μm compared with the sham controls (Figure 9C).

In addition, we observed significant decreases in branch points in the CA1 region of the hippocampus in CMF-treated animals (apical: $t = 9.46$, $p < .001$; basal: $t = 3.26$, $p < .05$; Table 2), ends (apical: $t = 11.35$, $p < .001$) but not in the basal ($t = 2.45$, $p = .07$; Table 2), and we observed significant decreases in the length of dendrites (apical: $t = 8.06$, $p < .001$; Table 2) but not in the basal ($t = 2.33$, $p = .08$; Table 2). Dendritic complexity was also significantly compromised by CMF treatment (apical: $t = 6.59$, $p < .01$; Figure 9B) but not in the basal ($t = 2.07$, $p < .06$) (Figure 9D).

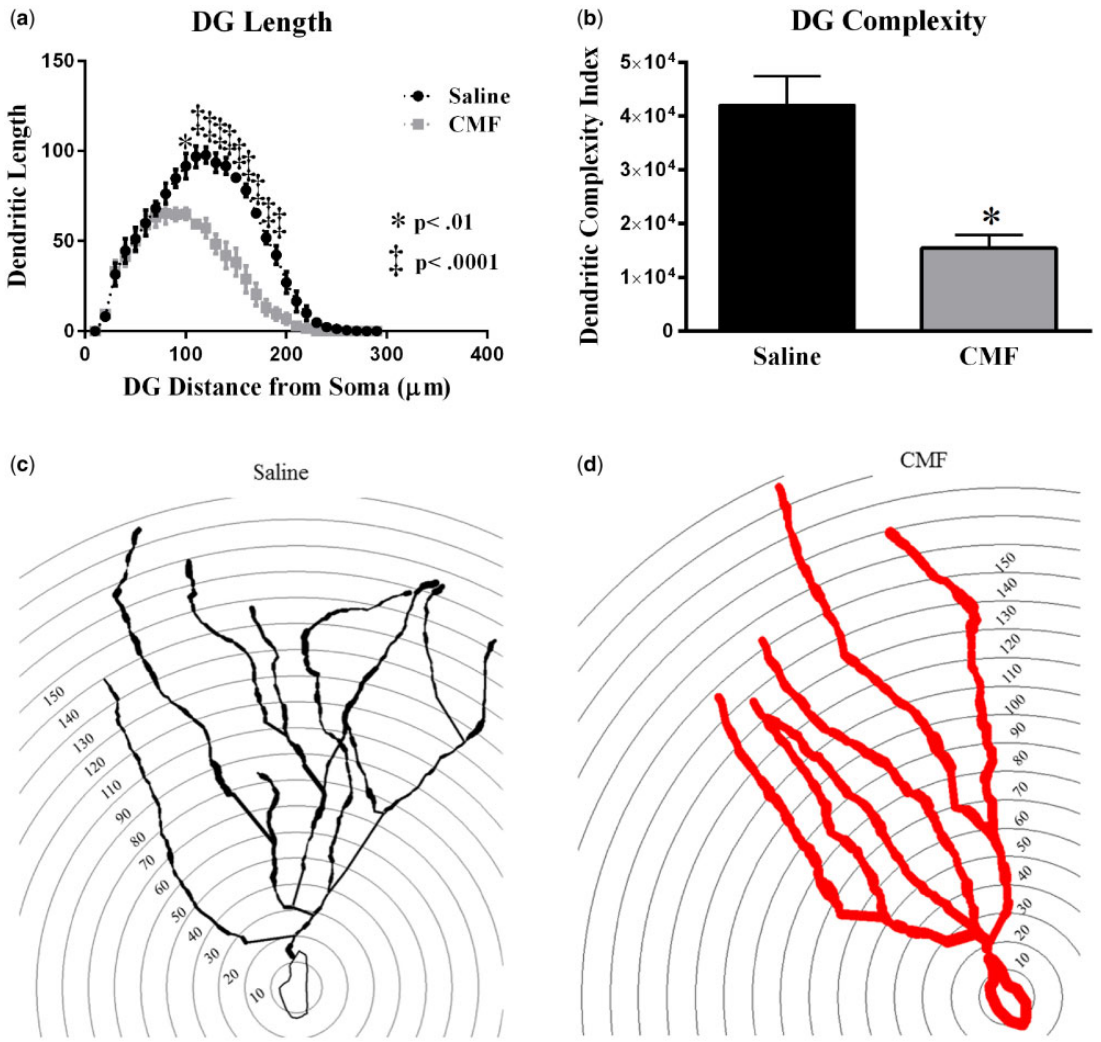

Figure 6. CMF- treatment significantly decreased dendritic complexity throughout the DG region of the hippocampus. a) Dendritic length measured by Sholl analysis revealed a decrease in arborization particularly evident at distances between 100-190 μm from the soma b) CMF-treatment significantly decreased complexity. (c-d) Representative tracings of DG granule neurons superimposed over concentric rings (10 μM) used for Sholl analysis. Average ± SEM ($n = 5$); * $P < .05$; ‡ $P < .001$.

CA3 pyramidal neurons. There was a significant interaction between treatment and segmental dendritic length in the CA3 apical areal ($F_{(25,\ 78)} = 11.80$, $p < .001$; Figure 10A). Two-way ANOVA revealed a significant main effect of CMF-treatment ($F_{(1,\ 124)} = 263.1$, $p < .001$) and an effect of length ($F_{(30,\ 124)} = 49.06$, $p < .001$). Further analysis with Holm-Sidak Post-hoc analysis showed CMF treatment decreased dendritic arborization 110-220 μm (Figure 10A) away from the soma when compared with saline treated controls.

In the basal dendrites of CA3 pyramidal cells, there was a significant interaction between treatment and sham segmental dendritic length ($F_{(30,\ 124)} = 8.65$; $p < .0001$; Figure 10C). The ANOVA also detected a main effect of treatment ($F_{(1,\ 124)} = 224.0$; $p < .0001$) and distance ($F_{(30,\ 124)} = 104.1$; $p < .0001$). Holm-Sidak Post-hoc analysis revealed that chemotherapy decreased dendritic arborization at 80–190 μm from the soma compared with the sham controls (Figure 10C).

Further, we observed significant changes in dendritic complexity in the CA3 region of the hippocampus. Branch points were significantly decreased in CMF-treated animals when compared with saline controls (apical: $t = 3.33$, $p < .01$; basal: $t = 6.83$, $p < .01$; Table 3). Dendrite length was compromised (apical: $t = 7.02$, $p < .01$; basal: $t = 4.86$, $p < .01$; Table 3), ends (apical: $t = 10.58$, $p < .001$; basal: $t = 5.52$, $p < .01$; Table 3) and the dendritic complexity was significantly reduced after CMF-treatment (apical: $t = 8.35$, $p < .01$; Figure 10B: $t = 7.78$, $p < .001$; Figure 10D).

Changes in Cytokine Production

Hippocampal homogenates from CMF-treated ($n = 5$) and saline-treated ($n = 5$) mice were tested to determine levels of 16 cytokines and chemokines using the Q-Plex Mouse Cytokine Screen. Cytokine levels decreased in CMF-treated animals compared with controls: IL-1α ($t = 2.71$, $p < .05$), IL-1β ($t = 2.44$, $p < .05$), IL-3 ($t = 2.71$, $p < .05$), IL-10 ($t = 2.47$, $p < .05$), and TNF-α ($t = 4.19$, $p < .01$) (Figure 1).

DISCUSSION

CMF: 2-Week Postchemotherapy

Half of BC patients are over 65 years old (Wefel et al., 2004), use of adult 6-month-old female mice was chosen to better represent a BC survivor. Additionally, research using female mice

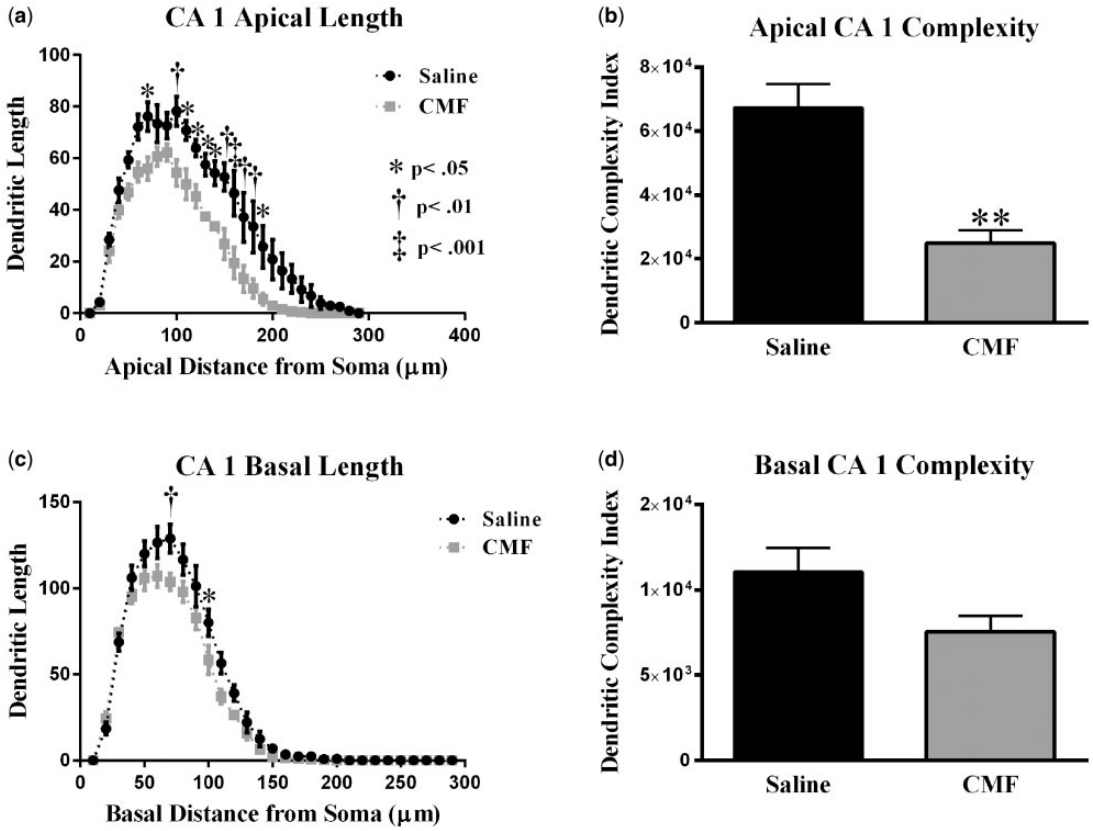

Figure 7. Sholl analyses of CA1 pyramidal neurons (a) Dendritic length measured by Sholl analysis in CA1 apical revealed a decrease in arborization at 70–130 μm from the soma after exposure to CMF. (b) CMF exposure greatly decreased overall dendrite complexity. (c) In the CA1 basal, mice exposed to CMF showed a decrease in arborization at 70 and 100 μm from the soma. (d) CMF exposure did not significantly decrease overall dendrite complexity in CA1 basal area. Average ± SEM ($n = 5$); * $P < .05$; ** $P < .01$; ‡ $P < .001$.

Table 1. Effects of CMF on Dendritic Morphology and Complexity in Hippocampal DG

Cell Type and Measurement DG	Saline (Mean ± SEM)	CMF (Mean ± SEM)	*p*-Value
Thin spines	60.04 ± 3.38	63.58 ± 1.45	$p = .93$
Stubby spines	**22.74 ± 1.82**	**29.75 ± 1.72**	$p < .05$
Mushroom spines	**14.42 ± 0.32**	**10.26 ± 0.16**	$p < .01$
Overall density	18.20 ± 0.18	18.38 ± 0.34	$p = 0.23$
Total dendritic length (μm)	**1219 ± 73.79**	**1747 ± 191.3**	$p < .001$
Total # ends	**11.14 ± .26**	**7.65 ± .35**	$p < .01$
Total # branch points	**10.25 ± 0.50**	**16.35 ± 2.45**	$p < .05$

Values in boldface are significant.

was chosen because female cancer survivors report a much higher incident of cognitive deficits following chemotherapy than males (Kohli et al., 2007). Mice at 2-week postchemotherapy exhibited no signs of deteriorating health, as food consumption and body weights were comparable across the duration of the 6-week study. This is congruent with previous work in our laboratory following CYP administration and unpublished data following CMF administration at other timepoints. CMF administration in rats found significant differences between CMF and control rats, but weights of CMF-treated rats did not significantly differ from their baseline (Briones and Woods, 2011). However, significant weight loss has been noted in previous work following larger chemotherapeutic doses (Aston et al., 2017; Fremouw et al., 2012).

The prevalence of acute and long-term cognitive impairments in BC survivors is well-documented, including deficits in learning, memory, attention, processing speed, and executive function. Deficits within the first 6 months are reported to affect from 48% to 95% of BC survivors (Ahles and Saykin, 2002), and a cross-sectional study totaling nearly 1500 BC survivors reported the incidence of cognitive deficits persisting 1- to 2-year postchemotherapy to range from 19% to 78% (Wefel and Schagen, 2012). For example, Schagen et al. identified deficits in BC survivors following adjuvant CMF treatment compared with age-matched BC survivors who did not receive adjuvant treatment. CMF-treated survivors had significantly poorer performance 2-year postchemotherapy in delayed verbal memory recall and both immediate and delayed visual memory recall (Schagen et al., 1999). In rats, CMF administration was found to impair long-term spatial memory 3-week postchemotherapy. In MWM probe trials, CMF-treated rats spent significantly less time swimming in the target quadrants compared with the other quadrants (Briones and Woods, 2011). Current *in vivo* literature following CMF, though limited, is congruent with our behavioral results, as long-term spatial memory impairment was identified in rodent models 2- to 3-week postchemotherapy. Cognitive deficits have been observed in hippocampal dependent tasks for animals treated with various chemotherapeutic agents. For example, monotherapy with CYP, MTX, and 5-FU

Table 2. Morphological Analysis of Apical and Basal Dendrites in CA1

Cell Type and Measurement	Saline (Mean ± SEM)	CMF (Mean ± SEM)	*p*-Value
CA1 apical			
Thin spines	56.50 ± 3.10	62.04 ± 2.07	$p = .17$
Stubby spines	30.07 ± 3.20	26.68 ± 1.58	$p = .37$
Mushroom spines	13.43 ± 1.04	11.28 ± 0.88	$p = .15$
Overall density	17.27 ± 0.38	18.90 ± 0.68	$p = .07$
Total dendritic length (μm)	**1031 ± 52.76**	**647.7 ± 41.91**	**$p < .001$**
Total # ends	**11.14 ± .26**	**7.65 ± .35**	**$p < .001$**
Total # branch points	**10.04 ± .33**	**6.52 ± .36**	**$p < .001$**
CA1 basal			
Thin spines	60.04 ± 3.38	63.58 ± 0.94	$p = .34$
Stubby spines	27.17 ± 2.82	25.97 ± 0.33	$p = .68$
Mushroom spines	13.03 ± 1.08	10.45 ± 0.66	$p = .08$
Overall density	**17.49 ± 0.39**	**19.80 ± 0.58**	**$p < .01$**
Total dendritic length (μm)	961.6 ± 29.19	821.7 ± 31.70	$p = .08$
Total # ends	11.52 ± 0.60	9.29 ± .52	$p = .07$
Total # branch points	**8.80 ± .56**	**5.7 ± .25**	**$p < .05$**

Values in Boldface are significant.

Table 3. Morphological Analysis of Apical and Basal Dendrites in CA3

Cell Type and Measurement	Saline (Mean ± SEM)	CMF (Mean ± SEM)	*p*-Value
CA3 apical			
Thin spines	58.69 ± 1.56	60.06 ± 1.34	$p = .52$
Stubby spines	27.72 ± 1.69	27.99 ± 1.50	$p = .90$
Mushroom spines	13.59 ± 0.57	11.95 ± 0.97	$p = .18$
Overall density	17.50 ± 0.59	18.53 ± 0.11	$p = .13$
Total dendritic length (μm)	**1684± 138.0**	**748.3 ± 63.66**	**$p < .01$**
Total # ends	**14.67 ± .82**	**6.64 ± .39**	**$p < .001$**
Total # branch points	**13.11± .75**	**10.04 ± .36**	**$p < .05$**
CA3 basal			
Thin spines	61.79 ± 1.82	60.39 ± 1.45	$p = .56$
Stubby spines	26.83 ± 1.33	27.88 ± 1.96	$p = .68$
Mushroom spines	11.37 ± .73	11.73 ± 1.10	$p = .79$
Overall density	**16.49 ± 1.25**	**20.60± 0.98**	**$p < .05$**
Total dendritic length (μm)	**1566 ± 103.9**	**907.4 ± 71.04**	**$p < .01$**
Total # ends	**15.18 ± 0.84**	**9.08 ± .52**	**$p < .01$**
Total # branch points	**12.50 ± .66**	**8.05 ± .56**	**$p < .01$**

administration has also revealed learning and memory deficits across several behavioral assays, including object recognition and MWM (Han et al., 2008; Seigers et al., 2008; Wigmore, 2013). Oxaliplatin administered in combination with 5-FU impaired NOR and spatial recognition memory (Fardell et al., 2012). One study found that rats showed impairments in conditioned aversion following six days of MTX administration (Madhyastha et al., 2002). Methotrexate in combination with 5-FU induced deficits in spatial (and nonspatial) learning and memory, associative learning, and discrimination learning (Winocur et al., 2012). Furthermore, mice that were co-administered MTX and 5-FU identified impaired learning in spatial memory, nonmatching to sample, and novel object recognition (Winocur et al., 2012). In contrast, some studies find no cognitive deficits post-chemotherapy. For example, monotherapy with CYP or 5-FU did not impair LTM in female rats at 7- or 29-week postchemotherapy (Lee et al., 2006). Combination treatment with CYP and 5-FU also did not result in LTM deficits in male rats 8-week postchemotherapy (Long et al., 2011). Though both of these studies were in rat models, which could indicate a species difference, neither study was a triple combination. It is possible the combination of CAF or CMF renders the hippocampus more vulnerable than single or double administration of CYP and/or 5-FU.

Spatial learning and memory in Y-Maze and MWM are behavioral tasks reliant upon hippocampal function (Morris et al., 1982, 1990; Moser et al., 1993; Shu et al., 2015). Since we identified impaired LTM in our CMF-treated mice, we chose to evaluate potential alterations in the dendritic architecture within the hippocampal tri-synaptic network (DG, CA1, and CA3) via Golgi-Cox staining. Dendritic architecture is intimately involved in learning and memory; and the extent and pattern of dendritic morphology can dictate the number of synaptic inputs (Jan and Jan, 2010). Dendritic spines are the specialized subcellular compartments which receive excitatory input within the CNS. Following calculations of overall spine density, we classified three morphological classes of dendritic spines: (1) mushroom spines, (2) stubby spines, and (3) thin spines. Spines are activity-dependent, as high-frequency stimulation induces spine development in hippocampal neurons (Maletic-Savatic et al., 1999). Thin spines, or "learning" spines, are transient and mobile; mushroom spines, or "memory" spines, are more stable and persist for months (Bourne and Harris, 2007; Kasai et al., 2003). For example, thin spines can either retract after a few days or develop into mushroom spines. Alternatively, the mushroom spines are relatively stable and can survive for an extended period. The strength of neuronal connections is thought to be based on the number of spines and/or their volume (Harris et al., 2003; Kasai et al., 2003; Leuner and Shors, 2013). In this study, we identified an increase in overall spine density within CA1 basal and CA3 basal dendrites, but there were no changes within the DG, CA1 apical, or CA3 apical dendrites. Regardless, spine classification following CMF administration in this study revealed increases in stubby spines and decreases in mushroom spines within the DG. These results directly mirror previous work in our laboratory assessing 5-FU administration in aged male mice where increases in stubby spines and decreases in mushroom spines were identified within the DG, CA1, and CA3 (Groves et al., 2017). Decreases in mushroom spines correlates with our foundational understanding of memory storage. In fact, a significant reduction in mushroom spines has also been identified in an Alzheimer's disease mouse model (Sun et al., 2014).

To further investigate the effects of CMF chemotherapy on neuronal morphology, a segmental Sholl analysis was performed to examine changes in dendritic length as a function of radial distance from the cell soma. Dendritic length, branch points, ends, and dendritic complexity were significantly decreased in CMF-treated mice. Literature supports these findings in that various other chemotherapeutic agents have also been found to alter dendritic branching and spine morphology. For example, overall loss in spine morphology and density following CYP administration was identified in rats who also exhibited diminished performance on hippocampal-reliant behavioral tasks. In the study by Acharya et al., significant changes in dendritic length and complexity were detected 30-day posttreatment. However, CYP had little impact on the number of dendritic branch points within the CA1-3 region (Acharya et al., 2015). Another study by Andres et al. identified low doses of

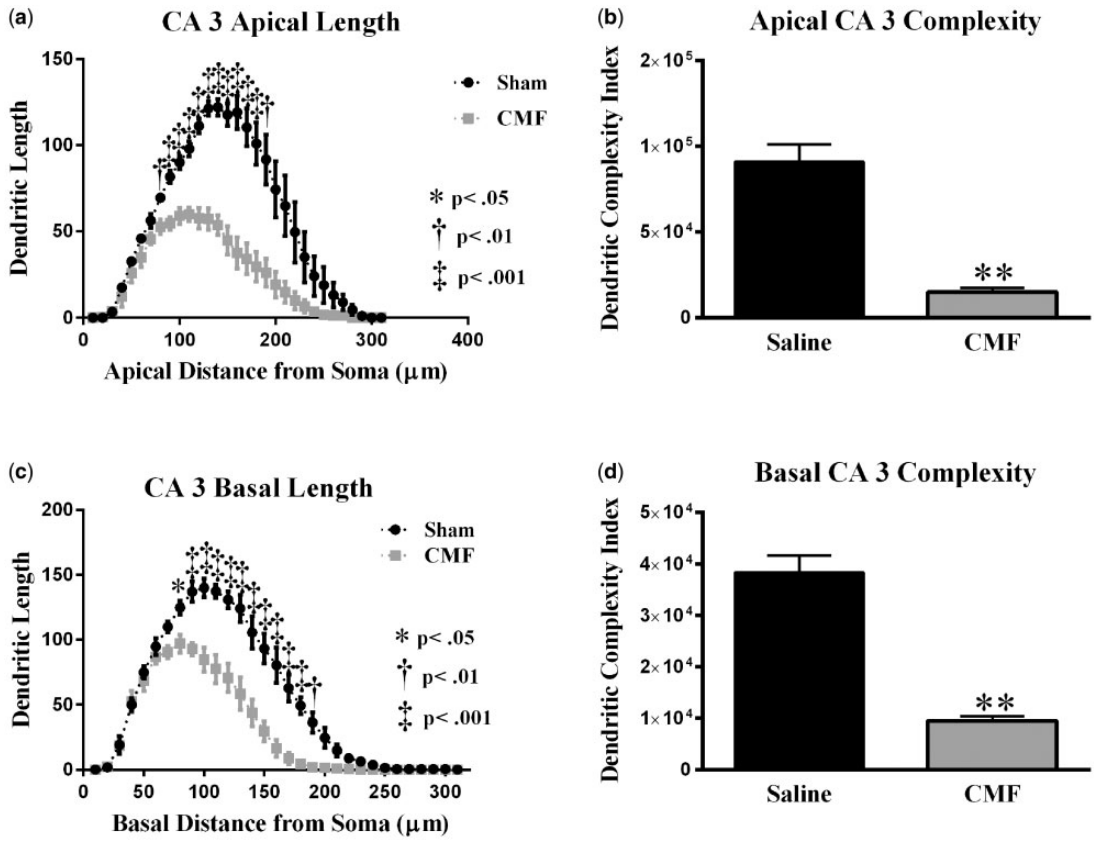

Figure 8. Analysis of dendritic complexity in CA3 apical region of CMF-treated mice versus saline-treated animals. (a) Dendritic length measured by Sholl analysis in CA3 apical revealed a decrease in arborization at 110–220 μm from the soma that was particularly evident after exposure to CMF. (b) CMF exposure greatly decreased overall dendritic complexity. (c) In the CA3 basal, mice exposed to CMF showed a decrease in arborization at 80–190 μm from the soma. (d) CMF exposure greatly decreased overall dendrite complexity in CA3 basal area. Average ± SEM ($n = 5$); * $P < .05$; ** $P < .01$; ‡ $P < .001$.

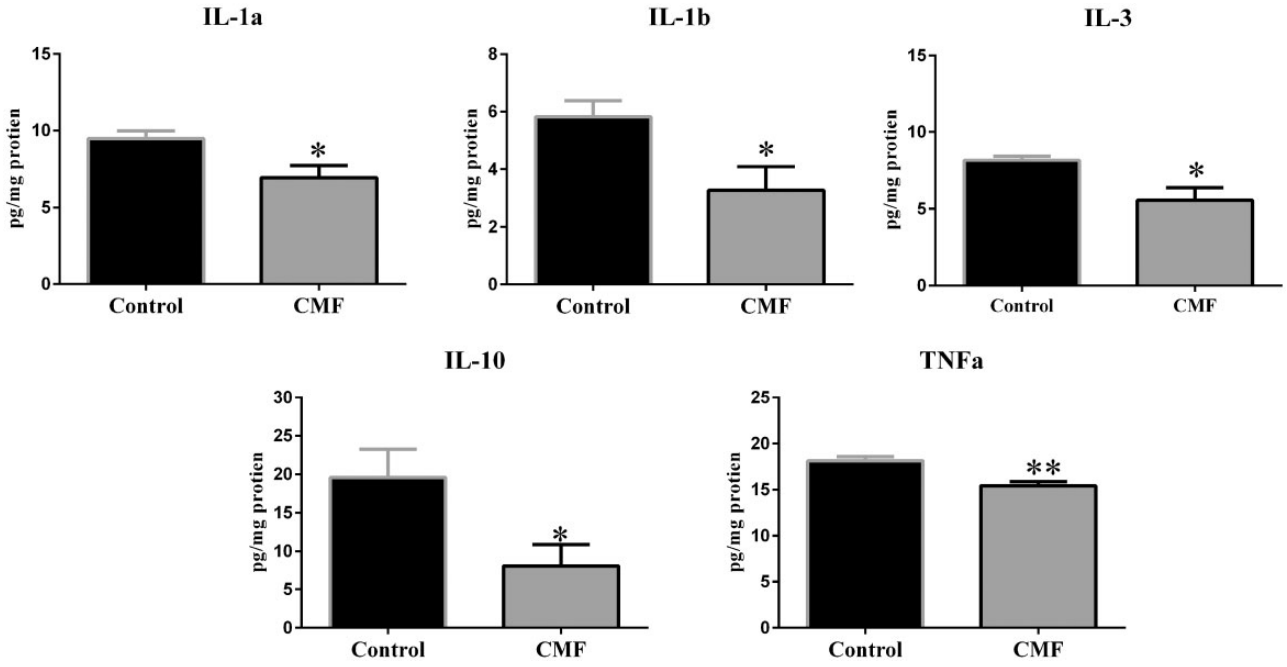

Figure 9. CMF treatment significantly decreased the amount of IL-1a, IL-1b, IL3, IL10 and TNF in the hippocampus. Each data point represents the mean of 5 mice; error bars are the SEM; * $P < .05$; ** $P < .01$.

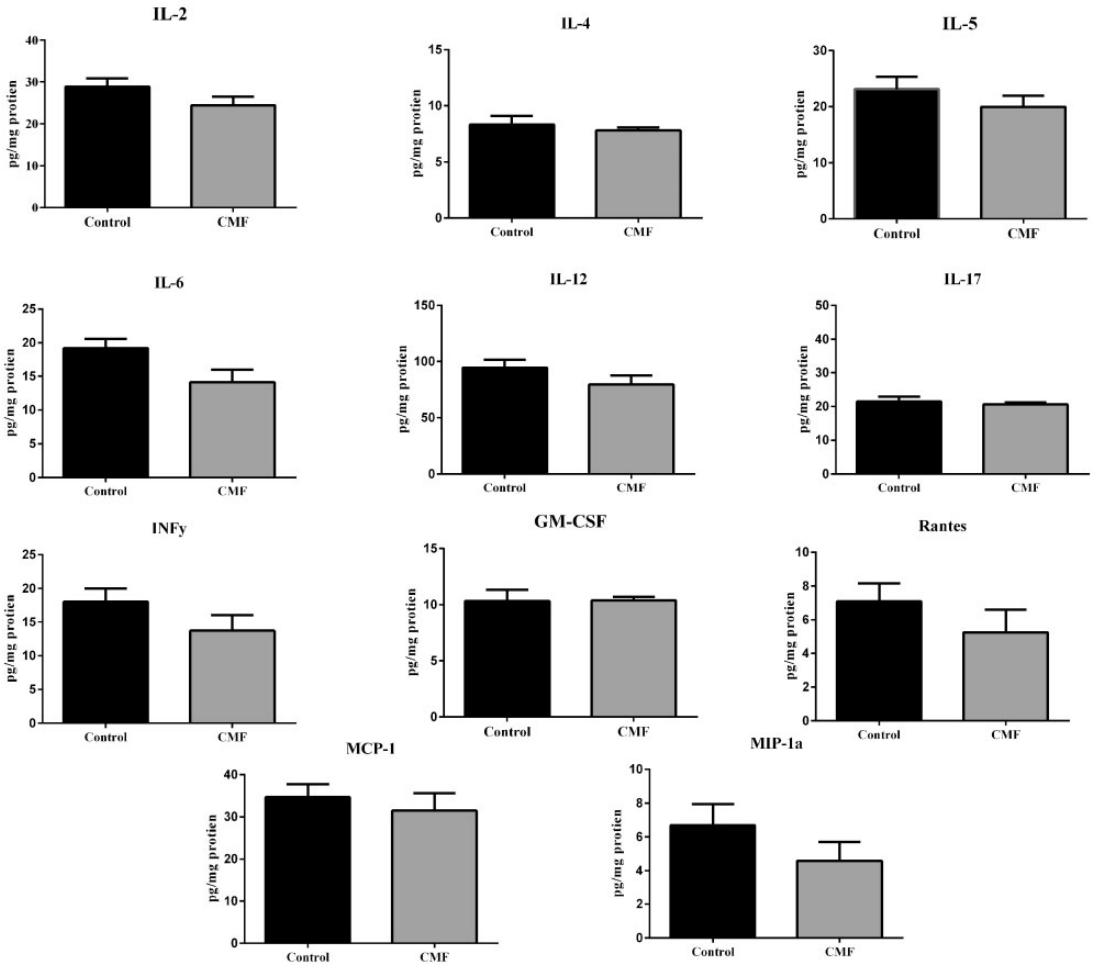

Figure 10. Cytokine and chemokine not significantly modulated by CMF treatment. Each data point represents the mean of 5 mice; error bars are the SEM.

Cisplatin caused a decrease in dendritic branching and complexity within CA1 (Andres et al., 2014). In our laboratory, alterations following 5-FU administration in aged mice also identified loss in dendritic length, branching, and complexity in the DG and CA1 (Groves et al., 2017).

Given the compromised hippocampal dendritic architecture coupled with LTM deficits, we chose to assess the levels of 16 cytokines and chemokines within the hippocampus to assess the role inflammation may play in CICIs. Dysregulation of cytokines has been identified in several disease states involving cognitive impairments (eg, Alzheimer's disease, Parkinson's disease, multiple sclerosis, and dementia) (Janelsins et al., 2012). Literature suggests dysregulation of cytokines in BC survivors may play a role in mediating cognitive impairments (Cheung et al., 2013; Cleeland et al., 2003). In our CMF-treated mice, we identified decreases in IL-1α, IL-1β, IL-3, IL-10, and TNF-α hippocampal levels.

Clinical data identified increased serum levels of IL-6, IL-8, and MCP-1 following CYP and doxorubicin (DOX) administration, with or without 5-FU; however, decreases in IL-6 were found following CMF (Janelsins et al., 2012). A subsequent study of various chemotherapy regimens found increases in TNF-α and decreases in IL-6 correlating with reduced hippocampal volumes and verbal memory impairments in BC survivors (Kesler et al., 2013). Other clinical data indicates increased IL-1β correlates with decreased response speed and increases in both IL-1β and IL-6 correlates to more self-perceived cognitive disturbances (Cheung et al., 2015). Cytokines play both crucial and complex roles in modulating learning and memory. For example, increased IL-1β can promote neuronal and oligodendrocyte death (Ramesh et al., 2013), inhibit the formation of hippocampal-dependent memory in rats (Cunningham et al., 1996), and cause spatial memory impairments in mice (Moore et al., 2009). Conversely, several studies have found IL-1β critical for learning and memory function (Donzis and Tronson, 2014). Evidently, the role of cytokines in modulating learning and memory are not fully realized as cytokines function through intricate network interactions yet to be fully elucidated (Boulanger et al., 2001; Pickering and O'Connor, 2007). *In vivo* studies assessing cytokine levels following chemotherapy are limited, but dysregulation of cytokines postchemotherapy has been identified. In rats, a single administration of MTX increased TNF-α in the peripheral tissue (Abdel-Raheem and Khedr, 2014). Our lab identified compromises in hippocampal dendritic complexity and increases in several hippocampal cytokines, including IL-1β and IL-3, following 5-FU treatment in aged male mice (Groves et al., 2017).

Cytokines have been traditionally be termed as pro- or anti-inflammatory, however cytokines are ultimately multifunctional proteins that work through complex networks often performing dual functions (Cavaillon, 2001). In congruence with our findings post-CMF, a recent collaboration within our lab

also found decreases in hippocampal levels of IL-1β, IL-6, and IL-12 in ovariectomized mice 10-week post-CYP and DOX administrations (Flanigan et al., 2018). A decrease in cytokines could be due to resultant cycling, as cytokine levels vary based on stress, fitness level, feeding state, and other individual dynamics (Monastero and Pentyala, 2017; Wang et al., 2010) or an effect exerted by MTX. In fact, Janelsin et al. identified decreased levels of pro-inflammatory cytokines in patients receiving CMF; however, increases in IL-6, IL-8, and MCP-1 were identified in both AC and CAF-treated patients (Janelsins et al., 2012). Methotrexate is a known cytokine suppressor and is prescribed for chronic inflammatory diseases, such as rheumatoid arthritis and psoriasis to stabilize high levels of T lymphocytes and cytokines (Gerards et al., 2003; Hagner and Joerger, 2010; Methotrexate, 2017). Furthermore, Seigers et al. determined that MTX administration in rats reduced hippocampal blood vessel density, had no effect on hippocampal cytokine levels, and reduced plasma cytokine levels (2010).

In the current study we observed decreased memory retention in behavioral paradigms for CMF-treated animals compared with controls. Data also indicates CMF compromises dendritic architecture and morphology within the hippocampus by 2-week postchemotherapy. In addition, we show that pro-inflammatory and anti-inflammatory cytokines were expressed in concentrations above control in mice exposed to CMF treated mice. In conclusion, chemotherapy-induced cognitive deficits can be transient or enduring obstacles for BC survivors. Continued research of short- and long-term chemotherapy-induced cognitive deficits are imperative to drive our current knowledge in the field. Measuring oxidative stress and other proposed mechanisms of cognitive decline will help us understand the manner in which this decline occurs and how it can be prevented.

DECLARATION OF CONFLICTING INTERESTS

The authors declared no potential conflicts of interest with respect to the research, authorship, and/or publication of this article.

FUNDING

This work was supported by Pilot Grant under NIH P20 GM109005 (ARA) and a grant from the Arkansas Breast Cancer Research Program. The funders had no role in study design, data collection and analysis, decision to publish, or preparation of the manuscript.

References

Abdel-Raheem, I. T., and Khedr, N. F. (2014). Renoprotective effects of montelukast, a cysteinyl leukotriene receptor antagonist, against methotrexate-induced kidney damage in rats. *Naunyn-Schmiedeberg's Arch. Pharmacol.* **387**, 341–353.

Acharya, M. M., Martirosian, V., Chmielewski, N. N., Hanna, N., Tran, K. K., Liao, A. C., Christie, L.-A., Parihar, V. K., and Limoli, C. L. (2015). Stem cell transplantation reverses chemotherapy-induced cognitive dysfunction. *Cancer Research* **75**, 676–686.

Ahles, T. A., and Saykin, A. J. (2002). Breast cancer chemotherapy-related cognitive dysfunction. *Clin. Breast Cancer* **3(Suppl. 3)**, S84–90.

Allen, A. R., Eilertson, K., Sharma, S., Baure, J., Allen, B., Leu, D., Rosi, S., Raber, J., Huang, T.-T., Fike, J. R., *et al.* (2014). Delayed administration of alpha-difluoromethylornithine prevents hippocampus-dependent cognitive impairment after single and combined injury in mice. *Radiat. Res.* **182**, 489–498.

Andres, A. L., Gong, X., Di, K., and Bota, D. A. (2014). Low-doses of cisplatin injure hippocampal synapses: A mechanism for 'chemo' brain? *Exp. Neurol.* **255**, 137–144.

Arnold, H., Bourseaux, F., and Brock, N. (1958). Chemotherapeutic action of a cyclic nitrogen mustard phosphamide ester (B 518-ASTA) in experimental tumours of the rat. *Nature* **181**, 931.

Aston, W. J., Hope, D. E., Nowak, A. K., Robinson, B. W., Lake, R. A., and Lesterhuis, W. J. (2017). A systematic investigation of the maximum tolerated dose of cytotoxic chemotherapy with and without supportive care in mice. *BMC Cancer* **17**, 684.

Awad, A., and Stuve, O. (2009). Cyclophosphamide in multiple sclerosis: Scientific rationale, history and novel treatment paradigms. *Ther. Adv. Neurol. Dis.* **2**, 50–61.

Benice, T., Rizk, A., Kohama, S., Pfankuch, T., and Raber, J. (2006). Sex-differences in age-related cognitive decline in C57BL/6J mice associated with increased brain microtubule-associated protein 2 and synaptophysin immunoreactivity. *Neuroscience* **137**, 413–423.

Boulanger, L. M., Huh, G. S., and Shatz, C. J. (2001). Neuronal plasticity and cellular immunity: Shared molecular mechanisms. *Curr. Opin. Neurobiol.* **11**, 568–578.

Bourne, J. N., and Harris, K. M. (2008). Balancing structure and function at hippocampal dendritic spines. *Annu. Rev. Neurosci.* **31**, 47–67.

Bourne, J., and Harris, K. M. (2007). Do thin spines learn to be mushroom spines that remember? *Curr. Opin. Neurobiol.* **17**, 381–386.

Briones, T. L., and Woods, J. (2011). Chemotherapy-induced cognitive impairment is associated with decreases in cell proliferation and histone modifications. *BMC Neuroscience* **12**, 124.

Briones, T. L., and Woods, J. (2014). Dysregulation in myelination mediated by persistent neuroinflammation: Possible mechanisms in chemotherapy-related cognitive impairment. *Brain Behav. Immun.* **35**, 23–32.

Carlson, R. W., Allred, D. C., Anderson, B. O., Burstein, H. J., Carter, W. B., Edge, S. B., Erban, J. K., Farrar, W. B., Goldstein, L. J., Gradishar, W. J., *et al.* (2009). Breast cancer. Clinical practice guidelines in oncology. *J. Natl. Compr. Canc. Netw.* **7**, 122–192.

Carrillo, E., Navarro, S. A., Ramírez, A., García, M. Á., Griñán-Lisón, C., Perán, M., and Marchal, J. A. (2015). 5-Fluorouracil derivatives: A patent review (2012–2014). *Expert. Opin. Ther. Pat.* **25**, 1131–1144.

Cavaillon, J. M. (2001). Pro- versus anti-inflammatory cytokines: Myth or reality. *Cell Mol. Biol. (Noisy-le-Grand)* **47**, 695–702.

Cheung, Y. T., Lim, S. R., Ho, H. K., and Chan, A. (2013). Cytokines as mediators of chemotherapy-associated cognitive changes: Current evidence, limitations and directions for future research. *PLoS One* **8**, e81234.

Cheung, Y. T., Ng, T., Shwe, M., Ho, H. K., Foo, K. M., Cham, M. T., Lee, J. A., Fan, G., Tan, Y. P., Yong, W. S., *et al.* (2015). Association of proinflammatory cytokines and chemotherapy-associated cognitive impairment in breast cancer patients: A multi-centered, prospective, cohort study. *Ann. Oncol.* **26**, 1446–1451.

Christakis, P. (2011). The birth of chemotherapy at Yale. Bicentennial lecture series: Surgery Grand Round. *Yale J. Biol. Med.* **84**, 169–172.

Cleeland, C. S., Bennett, G. J., Dantzer, R., Dougherty, P. M., Dunn, A. J., Meyers, C. A., Miller, A. H., Payne, R., Reuben, J. M.,

Wang, X. S., *et al.* (2003). Are the symptoms of cancer and cancer treatment due to a shared biologic mechanism? A cytokine-immunologic model of cancer symptoms. *Cancer* **97**, 2919–2925.

Cunningham, A. J., Murray, C. A., O'Neill, L. A., Lynch, M. A., and O'Connor, J. J. (1996). Interleukin-1 beta (IL-1 beta) and tumour necrosis factor (TNF) inhibit long-term potentiation in the rat dentate gyrus in vitro. *Neurosci. Lett.* **203**, 17–20.

de Jonge, M. E., Huitema, A. D., Rodenhuis, S., and Beijnen, J. H. (2005). Clinical pharmacokinetics of cyclophosphamide. *Clin. Pharmacokinet.* **44**, 1135–1164.

Dellu, F., Mayo, W., Cherkaoui, J., Le Moal, M., and Simon, H. (1992). A two-trial memory task with automated recording: Study in young and aged rats. *Brain Res.* **588**, 132–139.

DeSantis, C., Ma, J., Bryan, L., and Jemal, A. (2014). Breast cancer statistics, 2013. *CA Cancer J. Clin.* **64**, 52–62.

Diasio, R. B., and Harris, B. E. (1989). Clinical pharmacology of 5-fluorouracil. *Clin. Pharmacokinet.* **16**, 215–237.

Dietrich, J., Prust, M., and Kaiser, J. (2015). Chemotherapy, cognitive impairment and hippocampal toxicity. *Neuroscience* **309**, 224–232.

Dollery, C. T. (1999). *Therapeutic Drugs*, 2nd ed. Churchill Livingstone, Edinburgh, New York.

Donzis, E. J., and Tronson, N. C. (2014). Modulation of learning and memory by cytokines: Signaling mechanisms and long term consequences. *Neurobiol. Learn. Mem.* **115**, 68–77.

Dukic, S. F., Heurtaux, T., Kaltenbach, M. L., Hoizey, G., Lallemand, A., and Vistelle, R. (2000). Influence of schedule of administration on methotrexate penetration in brain tumours. *Eur. J. Cancer* **36**, 1578–1584.

Duschinsky, R., Pleven, E., and Heidelberger, C. (1957). The synthesis of 5-fluoropyrimidines. *J. Am. Chem. Soc.* **79**, 4559–4560.

Emadi, A., Jones, R. J., and Brodsky, R. A. (2009). Cyclophosphamide and cancer: Golden anniversary. *Nat. Rev. Clin. Oncol.* **6**, 638–647.

Fardell, J. E., Vardy, J., Shah, J. D., and Johnston, I. N. (2012). Cognitive impairments caused by oxaliplatin and 5-fluorouracil chemotherapy are ameliorated by physical activity. *Psychopharmacology (Berl)* **220**, 183–193.

Flanigan, T. J., Anderson, J. E., Elayan, I., Allen, A. R., and Ferguson, S. A. (2018). Effects of cyclophosphamide and/or doxorubicin in a murine model of postchemotherapy cognitive impairment. *Toxicol. Sci.* **162**, 462–474.

Fremouw, T., Fessler, C. L., Ferguson, R. J., and Burguete, Y. (2012). Preserved learning and memory in mice following chemotherapy: 5-Fluorouracil and doxorubicin single agent treatment, doxorubicin-cyclophosphamide combination treatment. *Behav. Brain Res.* **226**, 154–162.

Ganz, P. A., and Goodwin, P. J. (2015). Breast cancer survivorship: Where are we today? In *Improving Outcomes for Breast Cancer Survivors: Perspectives on Research Challenges and Opportunities*, p. 862

Genka, S., Deutsch, J., Stahle, P. L., Shetty, U. H., John, V., Robinson, C., Rapoport, S. I., and Greig, N. H. (1990). Brain and plasma pharmacokinetics and anticancer activities of cyclophosphamide and phosphoramide mustard in the rat. *Cancer Chemoth. Pharmacol.* **27**, 1–7.

Gerards, A. H., de, L. S., De, G. E., Dijkmans, B., and Aarden, L. (2003). Inhibition of cytokine production by methotrexate. Studies in healthy volunteers and patients with rheumatoid arthritis. *Rheumatology (Oxford)* **42**, 1189–1196.

Goodman, L. S., Wintrobe, M. M., *et al.* (1946). Nitrogen mustard therapy; use of methyl-bis (beta-chloroethyl) amine hydrochloride and tris (beta-chloroethyl) amine hydrochloride for Hodgkin's disease, lymphosarcoma, leukemia and certain allied and miscellaneous disorders. *J. Am. Med. Assoc.* **132**, 126–132.

Gottlieb, M., Leal-Campanario, R., Campos-Esparza, M. R., Sánchez-Gómez, M. V., Alberdi, E., Arranz, A., Delgado-García, J. M., Gruart, A., and Matute, C. (2006). Neuroprotection by two polyphenols following excitotoxicity and experimental ischemia. *Neurobiol. Dis.* **23**, 374–386.

Groves, T. R., Farris, R., Anderson, J. E., Alexander, T. C., Kiffer, F., Carter, G., Wang, J., Boerma, M., and Allen, A. R. (2017). 5-Fluorouracil chemotherapy upregulates cytokines and alters hippocampal dendritic complexity in aged mice. *Behav Brain Res.* **316**, 215–224.

Hagner, N., and Joerger, M. (2010). Cancer chemotherapy: Targeting folic acid synthesis. *Cancer Manag. Res.* **2**, 293–301.

Han, R., Yang, Y. M., Dietrich, J., Luebke, A., Mayer-Proschel, M., and Noble, M. (2008). Systemic 5-fluorouracil treatment causes a syndrome of delayed myelin destruction in the central nervous system. *J. Biol.* **7**, 12.

Harris, K. M. (1999). Structure, development, and plasticity of dendritic spines. *Curr. Opin. Neurobiol.* **9**, 343–348.

Harris, K. M., and Kater, S. B. (1994). Dendritic spines: Cellular specializations imparting both stability and flexibility to synaptic function. *Annu. Rev. Neurosci.* **17**, 341–371.

Harris, K. M., Fiala, J. C., and Ostroff, L. (2003). Structural changes at dendritic spine synapses during long-term potentiation. *Philos. Trans. R Soc. Lond. B Biol. Sci.* **358**, 745–748.

Hess, J. A., and Khasawneh, M. K. (2015). Cancer metabolism and oxidative stress: Insights into carcinogenesis and chemotherapy via the non-dihydrofolate reductase effects of methotrexate. *BBA Clin.* **3**, 152–161.

Honey, R. C., Watt, A., and Good, M. (1998). Hippocampal lesions disrupt an associative mismatch process. *J. Neurosci.* **18**, 2226–2230.

Jan, Y. N., and Jan, L. Y. (2010). Branching out: Mechanisms of dendritic arborization. *Nat. Rev. Neurosci.* **11**, 316–328.

Janelsins, M. C., Mustian, K. M., Palesh, O. G., Mohile, S. G., Peppone, L. J., Sprod, L. K., Heckler, C. E., Roscoe, J. A., Katz, A. W., Williams, J. P., *et al.* (2012). Differential expression of cytokines in breast cancer patients receiving different chemotherapies: Implications for cognitive impairment research. *Support. Care Cancer* **20**, 831–839.

Janelsins, M. C., Roscoe, J. A., Berg, M. J., Thompson, B. D., Gallagher, M. J., Morrow, G. R., Heckler, C. E., Jean-Pierre, P., Opanashuk, L. A., Gross, R. A., *et al.* (2010). IGF-1 partially restores chemotherapy-induced reductions in neural cell proliferation in adult C57BL/6 mice. *Cancer Inves.* **28**, 544–553.

Jean-Pierre, P., Johnson-Greene, D., and Burish, T. G. (2014). Neuropsychological care and rehabilitation of cancer patients with chemobrain: Strategies for evaluation and intervention development. *Support. Care Cancer* **22**, 2251–2260.

Kasai, H., Matsuzaki, M., Noguchi, J., Yasumatsu, N., and Nakahara, H. (2003). Structure-stability-function relationships of dendritic spines. *Trends Neurosci.* **26**, 360–368.

Kesler, S., Janelsins, M., Koovakkattu, D., *et al.* (2013). Reduced hippocampal volume and verbal memory performance associated with interleukin-6 and tumor necrosis factor-alpha levels in chemotherapy-treated breast cancer survivors. *Brain Behav. Immun.* **30(Suppl.)**, S109–116.

Kohli, S., Griggs, J. J., Roscoe, J. A., Jean-Pierre, P., Bole, C., Mustian, K. M., Hill, R., Smith, K., Gross, H., Morrow, G. R., *et al.* (2007). Self-reported cognitive impairment in patients with cancer. *J. Oncol. Pract.* **3**, 54–59.

Koppelmans, V., Breteler, M. M., Boogerd, W., Seynaeve, C., Gundy, C., and Schagen, S. B. (2012). Neuropsychological performance in survivors of breast cancer more than 20 years after adjuvant chemotherapy. *J. Clin. Oncol.* **30**, 1080–1086.

Lai, K. O., and Ip, N. Y. (2013). Structural plasticity of dendritic spines: The underlying mechanisms and its dysregulation in brain disorders. *Biochim. Biophys. Acta.* **1832**, 2257–2263.

Lee, G. D., Longo, D. L., Wang, Y., Rifkind, J. M., Abdul-Raman, L., Mamczarz, J. A., Duffy, K. B., Spangler, E. L., Taub, D. D., Mattson, M. P., *et al.* (2006). Transient improvement in cognitive function and synaptic plasticity in rats following cancer chemotherapy. *Clin. Cancer Res.* **12**, 198–205.

Leuner, B., and Shors, T. J. (2013). Stress, anxiety, and dendritic spines: What are the connections? *Neuroscience* **251**, 108–119.

Logan, R. M., Stringer, A. M., Bowen, J. M., Gibson, R. J., Sonis, S. T., and Keefe, D. M. (2008). Serum levels of NFkappaB and pro-inflammatory cytokines following administration of mucotoxic drugs. *Cancer Biol. Ther.* **7**, 1139–1145.

Long, J. M., Lee, G. D., Kelley-Bell, B., Spangler, E. L., Perez, E. J., Longo, D. L., de Cabo, R., Zou, S., and Rapp, P. R. (2011). Preserved learning and memory following 5-fluorouracil and cyclophosphamide treatment in rats. *Pharmacol. Biochem. Behav.* **100**, 205–211.

Longley, D. B., Harkin, D. P., and Johnston, P. G. (2003). 5-fluorouracil: Mechanisms of action and clinical strategies. *Nature Rev. Cancer.* **3**, 330–338.

Luznik, L., Jones, R. J., and Fuchs, E. J. (2010). High-dose cyclophosphamide for graft-versus-host disease prevention. *Curr. Opin. Hematol.* **17**, 493–499.

Lyons, L., Elbeltagy, M., Bennett, G., and Wigmore, P. (2011). The effects of cyclophosphamide on hippocampal cell proliferation and spatial working memory in rat. *PLoS One* **6**, e21445.

ELBeltagy, M., Mustafa, S., Umka, J., Lyons, L., Salman, A., Dormon, K., Allcock, C., Bennett, G., and Wigmore, P. (2012). The effect of 5-fluorouracil on the long term survival and proliferation of cells in the rat hippocampus. *Brain Res. Bull.* **88**, 514–518.

Madhyastha, S., Somayaji, S. N., Rao, M. S., Nalini, K., and Bairy, K. L. (2002). Hippocampal brain amines in methotrexate-induced learning and memory deficit. *Can. J. Physiol. Pharmacol.* **80**, 1076–1084.

Madondo, M. T., Quinn, M., and Plebanski, M. (2016). Low dose cyclophosphamide: Mechanisms of T cell modulation. *Cancer Treat. Rev.* **42**, 3–9.

Magariños, A. M., Li, C. J., Gal Toth, J., Bath, K. G., Jing, D., Lee, F. S., and McEwen, B. S. (2011). Effect of brain-derived neurotrophic factor haploinsufficiency on stress-induced remodeling of hippocampal neurons. *Hippocampus* **21**, 253–264.

Maletic-Savatic, M., Malinow, R., and Svoboda, K. (1999). Rapid dendritic morphogenesis in CA1 hippocampal dendrites induced by synaptic activity. *Science* **283**, 1923–1927.

Malouf, M., Grimley, E. J., and Areosa, S. A. (2003). Folic acid with or without vitamin B12 for cognition and dementia. *Cochrane Database Syst. Rev.* **4**, CD004514

Methotrexate. (2017). Available at: http://www.clinicalkey.com/. Accessed January 7, 2018.

Monastero, R. N., and Pentyala, S. (2017). Cytokines as biomarkers and their respective clinical cutoff levels. *Int. J. Inflam.* **2017**, 4309485.

Moore, A. H., Wu, M., Shaftel, S. S., Graham, K. A., and O'Banion, M. K. (2009). Sustained expression of interleukin-1beta in mouse hippocampus impairs spatial memory. *Neuroscience* **164**, 1484–1495.

Morris, R. G., Garrud, P., Rawlins, J. N., and O'Keefe, J. (1982). Place navigation impaired in rats with hippocampal lesions. *Nature* **297**, 681–683.

Morris, R., Schenk, F., Tweedie, F., and Jarrard, L. (1990). Ibotenate lesions of hippocampus and/or subiculum: Dissociating components of allocentric spatial learning. *Eur. J. Neurosci.* **2**, 1016–1028.

Moser, E., Moser, M.-B., and Andersen, P. (1993). Spatial learning impairment parallels the magnitude of dorsal hippocampal lesions, but is hardly present following ventral lesions. *J.Neurosci.* **13**, 3916–3925.

Motulsky, H. J., and Brown, R. E. (2006). Detecting outliers when fitting data with nonlinear regression—a new method based on robust nonlinear regression and the false discovery rate. *BMC Bioinformatics* **7**, 123.

Peddi, P. F., Peddi, S., Santos, E. S., and Morgensztern, D. (2014). Central nervous system toxicities of chemotherapeutic agents. *Expert. Rev. Anticancer Ther.* **14**, 857–863.

Pickering, M., and O'Connor, J. J. (2007). Pro-inflammatory cytokines and their effects in the dentate gyrus. *Prog. Brain Res.* **163**, 339–354.

Plesnila, N. (2016). The immune system in traumatic brain injury. *Curr. Opin. Pharmacol.* **26**, 110–117.

Ramesh, G., MacLean, A. G., and Philipp, M. T. (2013). Cytokines and chemokines at the crossroads of neuroinflammation, neurodegeneration, and neuropathic pain. *Mediators Inflamm.* **2013**, 1.

Ramlackhansingh, A. F., Brooks, D. J., Greenwood, R. J., Bose, S. K., Turkheimer, F. E., Kinnunen, K. M., Gentleman, S., Heckemann, R. A., Gunanayagam, K., Gelosa, G., *et al.* (2011). Inflammation after trauma: Microglial activation and traumatic brain injury. *Ann. Neurol.* **70**, 374–383.

Riehl, J.-L., and Brown, W. J. (1964). Acute cerebellar syndrome secondary to 5-fluorouracil therapy. *Neurology* **14**, 961–961.

Rutman, R. J., Cantarow, A., and Paschkis, K. E. (1954). Studies in 2-acetylaminofluorene carcinogenesis. III. The utilization of uracil-2-C14 by preneoplastic rat liver and rat hepatoma. *Cancer Res.***14**, 119–123.

Sakane, T., Yamashita, S., Yata, N., and Sezaki, H. (1999). Transnasal delivery of 5-fluorouracil to the brain in the rat. *J. Drug Target.* **7**, 233–240.

Schagen, S. B., van Dam, F. S., Muller, M. J., Boogerd, W., Lindeboom, J., and Bruning, P. F. (1999). Cognitive deficits after postoperative adjuvant chemotherapy for breast carcinoma. *Cancer* **85**, 640–650.

Seigers, R., Schagen, S., Beerling, W., Boogerd, W., Vantellingen, O., Vandam, F., Koolhaas, J., and Buwalda, B. (2008). Long-lasting suppression of hippocampal cell proliferation and impaired cognitive performance by methotrexate in the rat. *Behav. Brain Res.* **186**, 168–175.

Seigers, R., Timmermans, J., van der Horn, H. J., de Vries, E. F. J., Dierckx, R. A., Visser, L., Schagen, S. B., van Dam, F. S. A. M., Koolhaas, J. M., Buwalda, B., *et al.* (2010). Methotrexate reduces hippocampal blood vessel density and activates microglia in rats but does not elevate central cytokine release. *Behav. Brain Res.* **207**, 265–272.

Sholl, D. A. (1953). Dendritic organization in the neurons of the visual and motor cortices of the cat. *J Anat.* **87**, 387–406.

Shu, S.-Y., Jiang, G., Zeng, Q.-Y., Wang, B., Li, H., Ma, L., Steinbusch, H., Song, C., Chan, W.-Y., Chen, X.-H., *et al.* (2015). The marginal division of the striatum and hippocampus has different role and mechanism in learning and memory. *Mol. Neurobiol.* **51**, 827–839.

Spires-Jones, T. L., Kay, K., Matsouka, R., Rozkalne, A., Betensky, R. A., and Hyman, B. T. (2011). Calcineurin inhibition with systemic FK506 treatment increases dendritic branching and dendritic spine density in healthy adult mouse brain. *Neurosci Lett* **487**, 260–263.

Sun, S., Zhang, H., Liu, J., Popugaeva, E., Xu, N.-J., Feske, S., White, C. L., and Bezprozvanny, I. (2014). Reduced synaptic STIM2 expression and impaired store-operated calcium entry cause destabilization of mature spines in mutant presenilin mice. *Neuron* **82**, 79–93.

Tada, E., Parent, J. M., Lowenstein, D. H., and Fike, J. R. (2000). X-irradiation causes a prolonged reduction in cell proliferation in the dentate gyrus of adult rats. *Neuroscience* **99**, 33–41.

Titus, A. D. J., Shankaranarayana Rao, B. S., Harsha, H. N., Ramkumar, K., Srikumar, B. N., Singh, S. B., Chattarji, S., and Raju, T. R. (2007). Hypobaric hypoxia-induced dendritic atrophy of hippocampal neurons is associated with cognitive impairment in adult rats. *Neuroscience* **145**, 265–278.

Treatment of Solid Tumor Cancers with the Chemotherapy Drug Methotrexate (2014). Available at: https://www.cancer.gov/research/progress/discovery/methotrexate. Accessed January 6, 2018.

Vollala, V. R., Upadhya, S., and Nayak, S. (2011). Enhancement of basolateral amygdaloid neuronal dendritic arborization following Bacopa monniera extract treatment in adult rats. *Clinics (Sao Paulo)* **66**, 663–671.

Wang, Z., Chen, G., Zhu, W.-W., and Zhou, D. (2010). Activation of nuclear factor-erythroid 2-related factor 2 (Nrf2) in the basilar artery after subarachnoid hemorrhage in rats. *Ann. Clin. Lab. Sci.* **40**, 233–239.

Wefel, J. S., and Schagen, S. B. (2012). Chemotherapy-related cognitive dysfunction. *Curr. Neurol. Neurosci. Rep.* **12**, 267–275.

Wefel, J. S., Lenzi, R., Theriault, R., Buzdar, A. U., Cruickshank, S., and Meyers, C. A. (2004). 'Chemobrain' in breast carcinoma?: A prologue. *Cancer* **101**, 466–475.

Weiss, B. (2008). Chemobrain: A translational challenge for neurotoxicology. *Neurotoxicology* **29**, 891–898.

Wigmore, P. (2013). The effect of systemic chemotherapy on neurogenesis, plasticity and memory. *Curr. Top. Behav. Neurosci.* **15**, 211–240.

Wigmore, P. M., Mustafa, S., El-Beltagy, M., Lyons, L., Umka, J., and Bennett, G. (2010). Effects of 5-FU. *Adv. Exp. Med. Biol.* **678**, 157–164.

Winocur, G., Henkelman, M., Wojtowicz, J. M., Zhang, H., Binns, M. A., and Tannock, I. F. (2012). The effects of chemotherapy on cognitive function in a mouse model: A prospective study. *Clin. Cancer Res.* **18**, 3112–3121.

Yule, S. M., Price, L., Pearson, A. D., and Boddy, A. V. (1997). Cyclophosphamide and ifosfamide metabolites in the cerebrospinal fluid of children. *Clin. Cancer Res.* **3**, 1985–1992.